

# UNDERSTANDING THE EVOLUTION OF THE MARTIAN ATMOSPHERE THROUGH NITROGEN ISOTOPES

H. Pieris, B. M. Jakosky, *LASP, University of Colorado, Boulder, CO, USA (heshani.pieris@colorado.edu)*

## Introduction:

The  $^{14}\text{N}/^{15}\text{N}$  ratio of the Mars atmosphere was first measured by Viking and then later by the Mars Science Laboratory (MSL). MSL measured a  $^{14}\text{N}/^{15}\text{N}$  ratio of  $173 \pm 11$  which corresponds to an enrichment of 1.57 times the terrestrial value of the  $^{15}\text{N}$  isotope. This type of enrichment can only be explained by a significant loss of N to space, with the lighter isotope escaping more efficiently. A quantitative understanding requires analyzing all of the sources, sinks and exchanges of  $\text{N}_2$ . We employ the processes of sputtering, photochemical escape by dissociative recombination and photodissociation, and volcanic outgassing to understand the evolution of  $\text{N}_2$  through time. Sputtering and photochemical escape are isotopically selective escape processes that preferentially remove the lighter isotope creating an enrichment of  $^{15}\text{N}/^{14}\text{N}$ . We use a forward time-marching model starting at an initial abundance at 4.4 Gya in time steps of 1 Myr to calculate the  $\text{N}_2$  abundance and  $^{15}\text{N}/^{14}\text{N}$  enrichment through time. This first set of plots allow us to quantify the amount of  $\text{N}_2$  lost under varying  $\text{CO}_2$  histories and understand the evolution of  $\text{N}_2$  in the atmosphere through time. We also vary the initial  $\text{N}_2$  abundance, initial  $\text{CO}_2$  pressure and rate of loss or input of each process (by a constant multiplicative factor; i.e., rate factor) and explore which combinations of these parameters allow solutions that satisfy today's nitrogen composition and isotopic ratio of the Martian atmosphere.

A similar study of the Martian nitrogen abundance and isotopic evolution was recently published by Hu and Thomas (Nature, 2022). While this work does a thorough analysis of the nitrogen evolution models, our work expands on this by extending the evolutionary timeline from 3.8 Gya back to 4.4 Gya. We believe that observing the evolutionary models throughout this most stable period of the Martian atmosphere is key to obtaining a more complete picture of the early atmospheric environment of Mars. Our work, when completed, will also entail examining the effects of impact supply and loss processes (discussed further in the following section) which were not included in the model of Hu and Thomas, 2022.

## Box Model:

To investigate the evolution of the Martian atmosphere through nitrogen isotopes, we constructed a box model allowing simultaneous inputs and outputs of nitrogen gas into the atmosphere. As dis-

played in Figure 1, the processes that remove nitrogen from the atmosphere are sputtering, photochemical escape (dissociative recombination and photodissociation), impact erosion and formation of nitrates. Further, nitrogen can also be replenished in the atmosphere by volcanic outgassing, impact erosion of nitrates, and supply from incoming interplanetary dust particles (IDPs) and meteorites. This current model will only consider the processes of sputtering, photochemical escape and volcanic outgassing. The rest of the processes will be investigated in future continuation of this work.

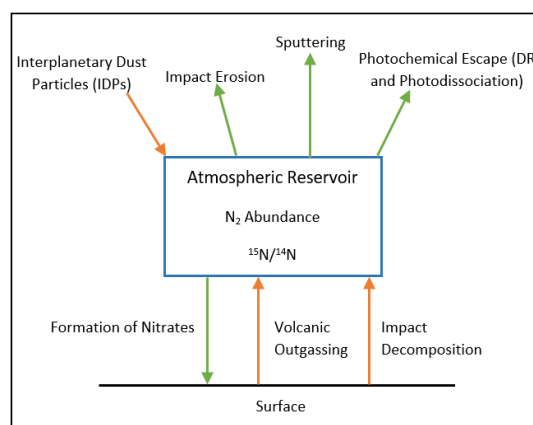


Figure 1: A schematic of the atmospheric reservoir and its exchanges with the surface and space. The green arrows portray the loss processes and the orange arrows represent the methods of replenishment.

## CO<sub>2</sub> History:

Escape rates of sputtering, dissociative recombination and photodissociation depend on the mixing ratio of  $\text{N}_2/\text{CO}_2$  in the bulk atmosphere. To account for the time varying abundance of  $\text{CO}_2$ , we employ two scenarios where the amount of  $\text{CO}_2$  in the atmosphere decays with a linear or with a power-law function. These two functions are set to begin at 3.8 Gya and decay to the present day  $\text{CO}_2$  partial pressure of 6 mbar. The power-law decay is of the form  $y = k \cdot x^a$ , where  $y$  is the  $\text{CO}_2$  abundance at each time,  $x$  is the time value and  $k$  and  $a$  are determined by the initial and final  $\text{CO}_2$  pressures.

In both of these evolution scenarios, we utilize a constant  $\text{CO}_2$  pressure for the time period of 4.4-3.8 Gya, as shown by Figure 2, in order to account for a stable atmosphere during the Noachian period. The initial  $\text{CO}_2$  pressures we employ for this study range as 6 mbar (assuming  $\text{CO}_2$  pressure has remained con-

stant over time), 10-100 mbar in increments of 10 mbar and 100-1000 mbar in increments of 100 mbar.

We use this simplified version of CO<sub>2</sub> decay in the atmosphere as an alternative to the more realistic approach of CO<sub>2</sub> loss which would entail studying the processes of escape to space by impacts, sputtering and photochemical loss, carbonate formation, and polar cap deposition alongside the loss processes of N<sub>2</sub>, which is beyond the scope of this project.

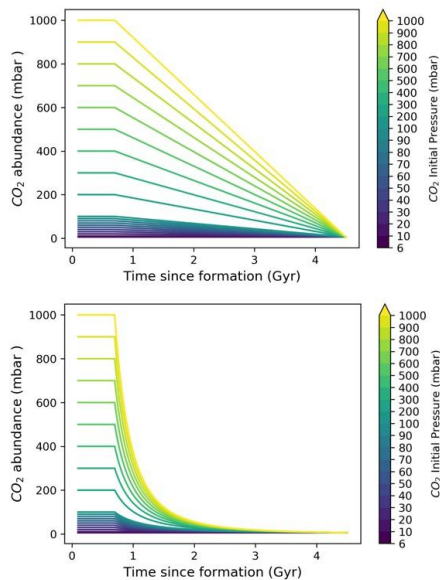


Figure 2: Linear and power-law decay of CO<sub>2</sub> with constant pressure through the Noachian epoch. The initial pressures vary from 6 mbar to 1000 mbar with all decaying to the current atmospheric pressure of 6 mbar.

### Input Parameters:

This box model takes inputs of initial N<sub>2</sub> abundance and initial CO<sub>2</sub> pressure. The initial N<sub>2</sub> abundance of the Martian atmosphere is not a value that is known since it is not plausible to measure this value in the current depleted atmosphere of Mars. For our analysis of the processes at some starting abundance, we use an initial value of  $\sim 9 \times 10^{42}$  molecules (108 mbar) which is the net abundance of the current N<sub>2</sub> budget of Earth's atmosphere scaled to the mass of Mars. Here, initial CO<sub>2</sub> pressure is set to vary from 6 mbar to 1 bar for both evolution histories of linear and power-law decay.

For the second set of plots, which explore the solutions that are able to reach today's nitrogen abundance and <sup>15</sup>N/<sup>14</sup>N ratio, the initial N<sub>2</sub> abundance is input as a free parameter. For this step of the model, we also introduce a rate factor, which is a multiplicative factor of the rate of each of the processes that varies over a set of values given as 0.25, 0.5, 1.0, 2.0, 5.0 and 10.0.

After the initial N<sub>2</sub> abundance is input into the model, an initial <sup>15</sup>N/<sup>14</sup>N ratio is used to obtain the

starting abundances of <sup>28</sup>N<sub>2</sub> and <sup>29</sup>N<sub>2</sub>. For this, we use the terrestrial <sup>15</sup>N/<sup>14</sup>N ratio of 0.00367 with the assumption that Earth has not undergone significant fractionation of nitrogen that would have resulted in the current ratio being an enrichment of its starting ratio

### Results:

We considered each process separately at first, in order to understand each one's behavior. After gaining this intuitive understanding, we included multiple processes simultaneously. Figure 3 portrays the simultaneous operation of all four processes of sputtering, dissociative recombination, photodissociation and volcanic outgassing starting at an initial N<sub>2</sub> abundance of 108 mbar at 4.4 Gya. Here, the CO<sub>2</sub> evolution follows a constant then power-law decay as shown by the bottom panel of Figure 2. It is clear that the highest N<sub>2</sub> loss occurs for lower initial CO<sub>2</sub> pressures and for higher initial pressures, there is a much less significant amount of N<sub>2</sub> lost through time. This occurs as a result of the escape rates being dependent on the N<sub>2</sub> mixing ratio which means that higher concentrations of CO<sub>2</sub> decrease N<sub>2</sub> escape. The sudden increase in N<sub>2</sub> abundance at  $\sim 1$ Gya seen for the lower pressure curves of 6 mbar and 10 mbar is caused by a sharp increase in volcanic outgassing at the early-Hesperian epoch. For lower initial CO<sub>2</sub> pressures, we see a steep initial decrease in the escape rates allowing volcanic outgassing to take precedence.

The bottom panel of Figure 3 shows that the lowest initial CO<sub>2</sub> pressure curves (6-20 mbar) have a rapid increase in enrichment within the first billion year, corresponding to the large decrease in N<sub>2</sub> abundances seen in the top panel. However, these peaks are short-lived and quickly reduce to arrive at an enrichment that falls below today's atmospheric measurements. Here the orange dashed lines represent the <sup>15</sup>N/<sup>14</sup>N measurement range within error bars made by Viking. We consider the value measured by Viking to allow room for slightly more uncertainty (Viking's 8.8% compared to Curiosity's 6.4% error). Under the specific assumptions of a CO<sub>2</sub> evolution of power-law decay and a starting N<sub>2</sub> abundance of 108 mbar, the N<sub>2</sub> evolution curves that are able to reach today's enrichment are those of 600 mbar - 1bar initial CO<sub>2</sub> pressure.

Figure 4 depicts the solutions that satisfy today's N<sub>2</sub> abundance and <sup>15</sup>N/<sup>14</sup>N enrichment ratio under varying initial N<sub>2</sub> values and rate factors of each process varying as 0.25, 0.5, 1.0, 2.0, 5.0 and 10.0. Here, the initial CO<sub>2</sub> pressure is set at 1 bar and decays under the power-law evolution scenario described by the bottom panel of Figure 2. The present-day range of N<sub>2</sub> pressure values are obtained by calculating a 30% seasonal variation of today's abun-

dance of  $\sim 0.125$  mbar, which provides a range from 0.0875 – 0.1625 mbar. This variation is an estimated consequence of seasonal  $\text{CO}_2$  condensation at the polar caps. According to this figure, the initial  $\text{N}_2$  pressures that are able to reach today's atmospheric conditions with an initial  $\text{CO}_2$  pressure of 1 bar, vary from 0.0005 mbar to 3 mbar. With volcanic outgassing being the sole process of  $\text{N}_2$  input assumed so far, solutions with lower initial  $\text{N}_2$  quickly rise to  $\sim 1$  mbar at which point they converge with the rest of the solutions to evolve to the present-day abundance. It should also be noted that this model was run for initial  $\text{CO}_2$  pressures of 6, 10 and 100 mbar as well (not shown here), and while the 100 mbar case had a few solutions that were able to satisfy today's composition there were none for 10 and 6 mbar.

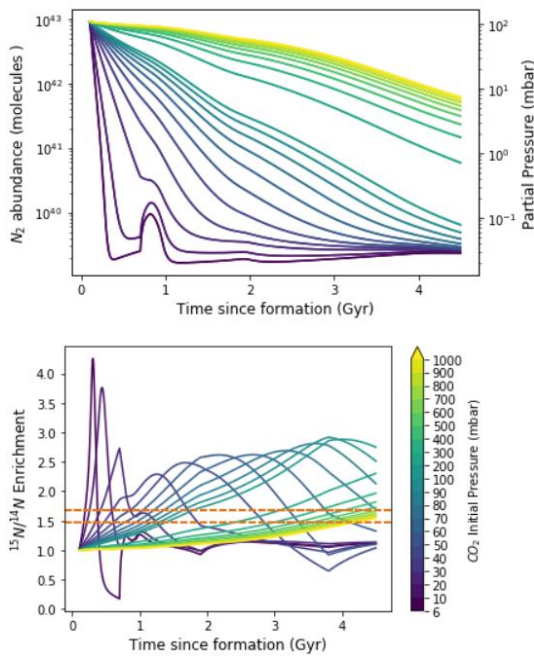


Figure 3:  $\text{N}_2$  abundance (top) and  $^{15}\text{N}/^{14}\text{N}$  enrichment (bottom) as a result of combining sputtering, photochemical escape and volcanic outgassing as  $\text{CO}_2$  decays in a power-law function after 3.8 Gya. The dashed orange lines describe the present day measured enrichment within error bars.

### Conclusions:

This current model employing the escape processes of sputtering, dissociative recombination and photodissociation and the input process of volcanic outgassing is able to produce solutions that satisfy the measured abundance and enrichment of  $\text{N}_2$  in today's Martian atmosphere. Under the assumption that only these four processes were in play in the evolution of nitrogen through time, the initial  $\text{N}_2$  pressure would have been in the range of 0.0005 mbar to 3 mbar. The initial converging of the solutions show that the scenarios that are able to reach

today's abundance are somewhat independent of the initial  $\text{N}_2$  abundance. A similar case in the enrichment plot shows that the different solutions that satisfy today's enrichment are independent of the  $^{15}\text{N}/^{14}\text{N}$  ratio up to 1 billion year after formation. As noted in the previous section, since the number of viable solutions decreased with decrease in initial  $\text{CO}_2$  pressures, it could be concluded that larger initial  $\text{CO}_2$  pressures ( $\sim 1$  bar or more) are a more likely depiction of the early atmospheric conditions of Mars.

Completion of this project will entail studying the evolution of  $\text{N}_2$  through time under all input and output processes described in Figure 1. This would allow us to obtain a more complete picture of the atmospheric evolution of Mars as well as a more accurate understanding of the initial atmospheric conditions at 4.4 Gya.

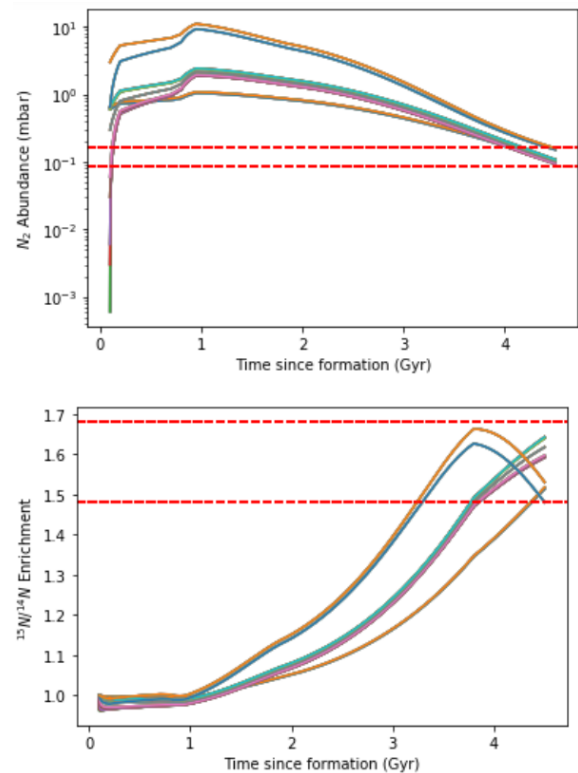


Figure 4:  $\text{N}_2$  abundance (top) and  $^{15}\text{N}/^{14}\text{N}$  enrichment (bottom) solutions that satisfy today's abundance and enrichment at an initial  $\text{CO}_2$  pressure of 1 bar. The dashed red lines depict the present day measured abundance and enrichment within error bars.